Chitin/silk fibroin/TiO2 bio-nanocomposite as a biocompatible wound dressing bandage with strong antimicrobial activity

Mojtaba Ghanbari Mehrabani, Ramin Karimian, Rasul Rakhshaei, Farzaneh Pakdel, Hosein Eslami, Vahid Fakhrzadeh, Mahdi Rahimi, Roya Salehi, Hossein Samadi Kafil

PII: S0141-8130(18)30706-2
DOI: doi:10.1016/j.ijbiomac.2018.05.102
Reference: BIOMAC 9703

To appear in:

Received date: 10 February 2018
Revised date: 4 May 2018
Accepted date: 15 May 2018

Please cite this article as: Mojtaba Ghanbari Mehrabani, Ramin Karimian, Rasul Rakhshaei, Farzaneh Pakdel, Hosein Eslami, Vahid Fakhrzadeh, Mahdi Rahimi, Roya Salehi, Hossein Samadi Kafil , Chitin/silk fibroin/TiO2 bio-nanocomposite as a biocompatible wound dressing bandage with strong antimicrobial activity. The address for the corresponding author was captured as affiliation for all authors. Please check if appropriate. Biomac(2017), doi:10.1016/j.ijbiomac.2018.05.102

Chitin/silk fibroin/TiO_2 bio-nanocomposite as a biocompatible wound dressing bandage with strong antimicrobial activity

Mojtaba Ghanbari Mehrabani[1, 2], Ramin Karimian[2*], Rasul Rakhshaei[3], Farzaneh Pakdel[4, 5], Hosein Eslami[5], Vahid Fakhrzadeh[5], Mahdi Rahimi[1, 3], Roya Salehi[1], Hossein Samadi Kafil[1**]

1. Drug Applied Research Center, Tabriz University of Medical Sciences, Tabriz, Iran
2. Chemical Injuries Research Center, Systems biology and poisonings institute, Baqiyatallah University of Medical Sciences, Tehran, Iran
3. Faculty of Chemistry, Department of Organic and Biochemistry, Tabriz University, Tabriz, Iran
4. Connective tissues Research Center, Tabriz University of Medical Sciences, Tabriz, Iran
5. Dental and Periodontal Research Center, Tabriz University of Medical Sciences, Tabriz, Iran

Corresponding authors:

***Ramin Karimian PhD:_karimian.r@gmail.com**

** **Hossein Samadi Kafil PhD: kafilhs@tbzmed.ac.ir**

Abstract

Interconnected microporous biodegradable and biocompatible chitin/silk fibroin/TiO_2 nanocomposite wound dressing with high antibacterial, blood clotting and mechanical strength properties were synthesized using freeze-drying method. The prepared nanocomposite dressings were characterized using SEM, FTIR, and XRD analysis. The prepared nanocomposite dressings showed high porosity above 90% with well-defined interconnected porous construction. Swelling and water uptake of the dressing were 93%, which is great for wound dressing applications. Haemostatic potential of the prepared dressings was studied and the results proved the higher blood clotting ability of the nanocomposites compared to pure components and commercially available products. Besides, cell viability, attachment and proliferation by MTT assay and DAPI staining on HFFF2 cell as a Human Caucasian Foetal Foreskin Fibroblast proved the cytocompatibility nature of the nanocomposite scaffolds with well improved proliferation and cell attachment. To determine the antimicrobial efficiencies, both disc diffusion method and colony counts were performed and results imply that nanocomposite scaffolds have high antimicrobial activity and could successfully inhibit the growth of *E. coli*, *S. aureus*, and *C. albicans*. Moreover, based on these results, the prepared chitin/silk fibroin/TiO_2 nanocomposite dressing could serve as a kind of promising wound dressing with great antibacterial and antifungal properties.

Keywords: antibacterial, antifungal, cytocompatibility, infection, silk fibroin, wound dressing.

1. Introduction

Epidermal tissue injuries are common in our daily life and cause serious problems; therefore, dressing these injuries with bandages could be help for wound healing. Cause exudate formation, improper collagen deposition delay the wound healing which are the major problems in the wound care process [1, 2]. Microbes are the most important reason of the wound infection [3, 4]. They can instantly grow and form colonies on the wound site and penetrate into deeper layers of the tissue causing internal infections [5]. In this regard, wound dressings are the most promising materials in wound care and play a major role in wound healing process. Ideal dressings should have several advantages such as biocompatibility, easily removing, maintaining moisture, absorbing wound exudate, and oxygen and water vapor permeability with antibacterial properties. They could protect the wounds from penetration of microorganisms, side-infection, maintaining a moist environment for skin wound healing, and bacterial invasion [6]. A wound dressing with antibacterial properties can help protect wound from infections and accelerate healing [7, 8].

Natural polymers are biocompatible and biodegradable and hence are very appropriate for biomedical applications [9]. Due to its great mechanical properties, biocompatibility, and low inflammatory, silk is one of the best natural biopolymers for wound dressing [10, 11]. Silk is basically composed of 70-80% hydrophobic fibroin and 30-20% hydrophilic sericin [12]. Sericin is a glue like water soluble protein encompassing fibroin and can be removed by a thermo-chemical treatment [13]. Silk fibroin is a natural fibrous protein and responsible for the mechanical strength of the silk [14]. Due to its abundance, high biocompatibility and biodegradability silk fibroin is widely used in biomedical applications such as wound dressing. However, its solubility restricts its applications [15, 16].

Chitin (β-(1, 4)-poly-*N*-acetyl-D-glucosamine) is the second most abundant polysaccharide after cellulose on the earth [17]. Its main sources are crabs, shrimps, lobsters, etc. [18]. Chitin occurs in three polymorphic crystalline forms of α, β and γ [19]. The crystalline structure of chitin determines its properties [20]. Chitin and its most important derivative chitosan, are widely used for wound dressing in different forms like hydrogel, scaffold fiber etc. [17, 21-23]. It has proven that chitin and chitosan leads to keratinocytes migration to the wound site, enhancing wound healing [24]. It has hemostatic, blood clotting, antibacterial and anti-inflammatory properties [25, 26].

At neutral pH chitin does not have antibacterial properties [27, 28]. To reach effective antibacterial properties some antibacterial agents should be added to it [29-32]. In recent years, many evidences demonstrated the potential antibacterial properties of non-toxic, long-lasting, and inexpensive titanium dioxide (TiO_2) nanoparticles [33, 34]. Silk fibroin (SF) nanofibrous mats were fabricated via electrospinning process and they were blended with TiO_2 nanoparticles [35]. These SF/TiO_2 nanofibrous mats exhibited antibacterial properties, with higher equilibrium water content and water vapor transmission rate than hydrocolloid dressing. Freeze-dried porous nanocomposite scaffolds were prepared from silk fibroin and titanium dioxide (TiO_2) nanoparticles as a bioactive reinforcing agent by a phase separation method [36]. TiO_2 nanoparticles resulted to an improvement of the mechanical strength. Antibacterial activity of chitosan/TiO_2 nanocomposite against Xanthomonas oryzae pv. oryzae was studied and the results showed antibacterial activity in both light and dark. [37]. Scaffolds composing of silk fibroin and TiO_2 nanoparticles fabricated using a salt-leaching process [38]. The resultant mechanical property of scaffolds was improved upon the introduction of TiO_2 NPs.

In this work, biodegradable and biocompatible chitin/silk fibroin/TiO_2 nanocomposite microporous and flexible bandages were created through a simple and inexpensive method compared to other methods like electrospinning. The role of TiO_2 nanoparticles on antibacterial and structural properties of the prepared microporous bandages was evaluated.

2. Material and Methods

2.1. Materials

Silk fibroin was extracted from Bombyx Mori silk cocoons purchased from Silk Worm Research Center of Iran. α-Chitin was purchased from Nano Novin Polymer Corporation (Iran). TiO_2 nano-powder with particle size of 10-25 nm was purchased from US Research Nanomaterials (Stock number: US3490, CAS number: 13463-67-7). Chicken egg white lysozyme was purchased from SIGMA (protein ≥90 %, ≥40,000 units/mg protein, L6876). Calcium Alginate Dressing with brand name KALTOSTAT was purchased from ChitoTech. DAPI (4,6-diamidino-2-phenylindole) was obtained from SIGMA (D9542). The normal human dermal fibroblast cell (HFFF2) was purchased from Pasteur Institute of Iran, Tehran, Iran. DMEM was purchased from Bio-Idea. Gentamicin and Fluconazole was purchased from ZAHRAVI Pharm. Co. Mueller Hinton Agar (MHA) was purchased from Liofilchem. *E. coli* (ATCC 25922) and *S. aureus* (ATCC 25923) strains were used. All other materials were purchased from Merck.

2.2. Characterization

Samples were lyophilized using a laboratory freeze-dryer instrument (martin christ alpha 1-4). The prepared samples were characterized using X-ray diffraction (XRD) (GNR (MPD-3000) (GNR model MPD-3000, Cu Kα radiation, operating at a voltage of 40 kV, 30mA, λ = 1.5 A°), Fourier transform infrared spectroscopy (FTIR) (Bruker-Tensor, model 270), and UV/VIS

spectroscopy (T70+ UV/VIS spectrometer PG instruments Ltd). The morphology of the prepared samples was characterized using scanning electron microscopy (SEM) (TESCAN 5001, Japan).

2.3. Extraction of Silk fibroin

Silk fibroin was extracted from Bombyx Mori cocoon. At first, cocoons were cut and heated in boiling 0.02 M Na_2CO_3 solution for 30 min to remove sericin protein. Remained Na_2CO_3 was removed by distilled water washing for several times then the sample was dried at 50 °C overnight. Degummed silk (SF) was dissolved in a ternary solvent system of $CaCl_2$/EtOH/H_2O (1/2/8 in molar ratio) at 70 °C for 4-5 h. After dialysis with cellulose tubular membrane (250-7u, Sigma) in deionized water for 3 days, the silk fibroin solution was centrifuged at 12000 rpm for 10 min. Gravimetric analysis showed the concentration of the final solution was 2.5 % w/v.

2.4. Preparation of Chitin/silk fibroin/TiO_2 dressing

The 2.5 w/v % chitin solution was prepared by dissolving the purified chitin powder in 11 w/v % NaOH and 4 w/v % urea solvent through the freezing/thawing method. An equal volume of the prepared silk fibroin solution (2.5 w/v %) was added to chitin solution to prepare a 50:50 v/v % chitin/silk fibroin solution. Glycerol as plasticizer (50 w/w %, weight of glycerol to the weight of chitin and silk fibroin in the solution) was added to the solution. The solution was mixed for 12 h at room temperature. Predetermined amount of TiO_2 nanoparticles (TiO_2 NPs) was dispersed in appropriate volume of distilled water using probe type sonicator. The resulted slurry was added to the chitin/silk fibroin solution to prepare 0.5, 1.5, 3.0 w/w % (weight of TiO_2 NPs to the weight of chitin/silk fibroin) nanocomposites and samples were denoted as S (silk fibroin), C (chitin), S+C (silk fibroin and chitin blend), T0.5, T1.5, T3.0 . The solution was mixed for another 24 h and then 0.25% (v/v) glutaraldehyde was added drop wise in 1:32 ratio (5 h) as the

crosslinking agent. The resulted paste was frozen at -20 °C for 12 h and freeze-dried at -70 °C for 48 h (Fig 1) to obtain 3D nanocomposite scaffolds as wound dressing bandage.

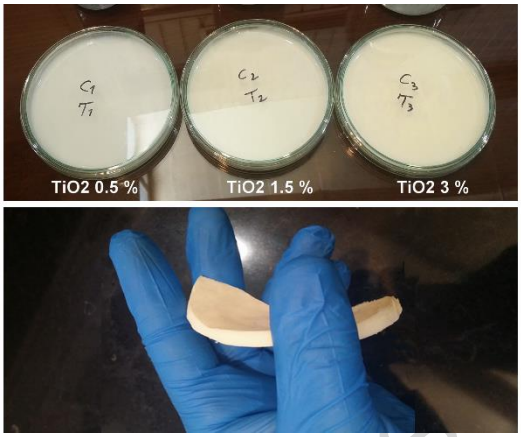

Fig. 1 Photographs of the prepared 3D nanocomposite scaffolds as wound dressing bandage.

2.5 Porosity and Density

Pore size and porosity of the prepared nanocomposites were determined using SEM images and "Image J" software. Four different images with different magnifications were used for each sample. The software separated pores and Feret diameter were calculate for the pores. To determine the density and porosity of the prepared samples we used a previously reported method based on the Archimedes rule [39]. Suitable volume of normal hexane was poured into a container. The weight of the n-hexane and container was determined (W_1). The predetermined weight of the sample (W_s) was immersed in normal hexane. After completely saturation of the sample the weight of the container was determined (W_2). Then n-hexane saturated sample was removed carefully and the container was weighed again (W_3). The volume of the sample (V_s), the volume of the pores (V_p), the density of the samples (ρ_s) and the porosity of the samples (ε) were calculated using formulas ($\rho_n = n.hex\ density = 654.8\ \left({}^{mg}/_{ml}\right)$):

$$V_S = {(W_2 - W_3 - W_S)}/{\rho_n}$$

$$V_P = {(W_1 - W_2 + W_S)}/{\rho_n}$$

$$\rho_S = {W_S\,\rho_n}/{(W_1 - W_2 + W_S)} = {W_S}/{V_S}$$

$$\varepsilon = {(W_2 - W_3 - W_S)}/{(W_1 - W_3)} = {V_P}/{(V_P + V_S)}$$

2.6 Swelling Ratio

To determine the degree of swelling of the prepared dressings, accurately weighed (W_d) samples with equal sizes were immersed in 1 × PBS (phosphate buffered saline) at physiological temperature and pH. At predetermined time intervals (1, 7, 14 and 21 h) the samples were taken out and blotted onto filter paper to remove surface water and then weighed (W_w). The degree of swelling (DS) was calculated using:

$$\mathrm{DS} = \frac{W_w - W_d}{W_d} \times 100$$

2.7 *In-vitro* biodegradation

To study biodegradation, the samples were accurately weighed (W_i) and immersed in PBS containing lysozyme (10000 U/ml) and incubated at 37 °C for 21 days. After 7, 14 and 21 days samples were taken out and washed with deionized water to remove absorbed ions. Then samples were freeze-dried and weighed (W_f).

$$Degradation\ (\%) = \frac{W_i - W_f}{W_i} \times 100$$

2.8 Mechanical Properties Evaluation

Tensile strength (TS) and elongation at break (EB) of the prepared nanocomposite dressings were evaluated using a universal testing machine (SANTAM, Model STM-1) at a crosshead speed of 0.5 and 40 mm min^{-1} with a 20 kg load cell (Bongshin, Model DBBP-20). According to D 3039/D 3039M standard, the measurements were carried out in a standard laboratory atmosphere (23 ± 3°C and 50 ± 10% relative humidity). The scaffold specimens were prepared with dimensions of 6 cm × 0.5 cm × 0.4 cm. Both ends of tensile specimens were clipped with a special gripper. Thickness of the samples was determined through measuring thickness of three different points of each sample. The experiment was carried out in triplicates.

2.9 *In-vitro* blood compatibility

The blood-clotting index (BCI) of the nanocomposite prepared dressings were tested and compared with commercially available dressing (Kaltostat, Convatec). Using an ulnar vein BD Discardit II sterile syringe human blood was drawn. The blood was mixed with sodium citrate and dextrose at a ratio of 1 to 9 as anticoagulant agent. The test was triplicated for this study and blood without sample was used as negative control. In a 25 ml plastic petri dish, 400 µl blood was added to each dressing. To start coagulation, 40 µl $CaCl_2$ solution (0.2 M) was added and samples were incubated at 37 °C for 10 min. 15 ml distilled water was added dropwise carefully. Afterward, 10 ml of the resulted solution was taken out and centrifuged at 1000 rpm for 1 min. The resulted supernatant was collected and incubated at 37 °C for 1 h. 200 µl of the solution was transferred to a 96 well plate (Fig.2). Optical density was determined at 540 nm by a BioTek reader using this formula:

$$\mathrm{BCI} = \frac{\mathrm{OD}_{\mathrm{sample}}}{\mathrm{OD}_{\mathrm{control}}} \times 100$$

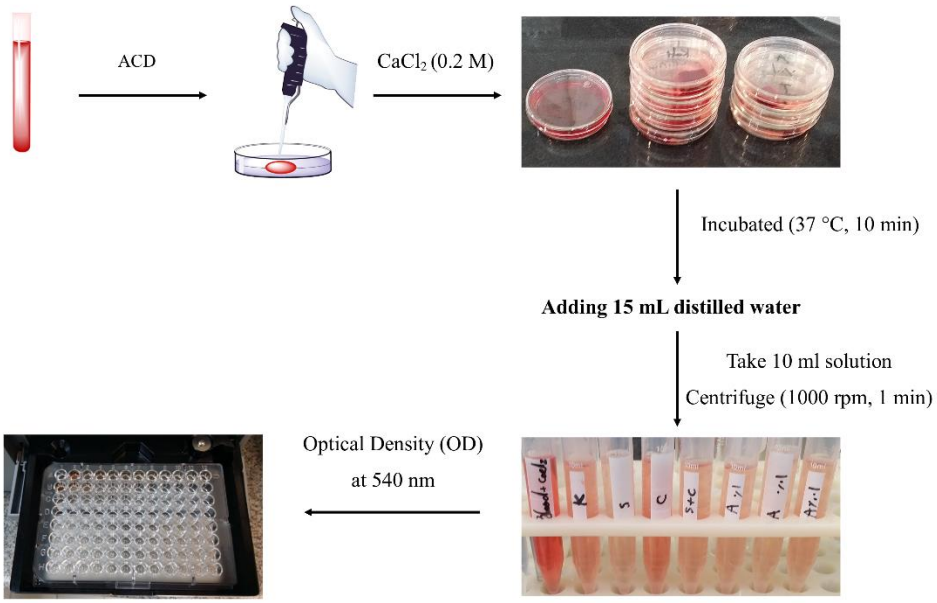

Fig.2 Overall sequence of steps in blood clotting evaluation

2.10 *In-vitro* Antibacterial and Antifungal Activity Evaluation

Antibacterial and antifungal activity of the prepared dressings was tested using Kirby-Bauer disk diffusion and colony count methods [40, 41]. *S. auresus* and *E. coli* were used as gram positive and gram negative strains respectively. *C. albicans* was used as fungal strain. In Kirby-Bauer disk diffusion method, Muller-Hilton agar for bacterial strains and Muller-Hilton agar congaing 2 % glucose for fungal strain were used as culturing media. 1 cm disk of each sample was prepared and sterilized using UV radiation. Disks were placed on previously inoculated medium. 25 µl of DMSO was added to the disks to improve the contact of the samples and medium. The plates were incubated for 24 h at 37 °C [42]. Then the inhibition zone around disks were determined. Positive controls of the bacterial and fungal strains were disks containing 10 µl Gentamicin and 25 µl Fluconazole, respectively. Negative controls were pure chitin, pure silk fibroin, and chitin/silk fibroin composite. In colony counting method, strains were cultured in Luria-Bertani broth (L.B broth) and incubated at 37 °C overnight. The concentration of bacteria

was 10^6 colony-forming units per milliliter (CFU/mL). UV sterilized disks were added to the L.B broth and incubated at 37 °C for 24 h. After the incubation period, the quantification of viable bacteria was made by serial dilution of the bacteria culture in normal saline followed by plating on LB agar plate for bacterial strains and Sabouraud Dextrose Agar (SDA) for fungal strain.

2.11 *In-vitro* evaluation of cytotoxicity

The MTT test was used as a sign of relative cell viability. The normal human dermal fibroblast (HFFF2) cells were served to estimate the *in-vitro* cytotoxicity of the extractions. The passaged (cells less than passage 7) and isolated cells were trypsinised, pilled and re-suspended in a known amount of DMEM media (high glucose). The cell concentration of 1×10^4 cells/mL was transferred onto 96-well tissue culture plates overnight. The samples were sterilized by placing in ethanol, and this was followed by UV irradiation for 30 minutes. The bandages (1 cm × 1 cm × 1 cm) were immersed in separate sterile tubes with 5 mL DMEM solution and incubated at 37 °C for 24 h. To examine the *in-vitro* cytotoxicity of the extractions, 4-mL extraction of each sample was collected. The culture media were changed with the extraction every two days. MTT assay was managed in 24 and 48 hours by changing the media with MTT solution in the wells for 4 h. The MTT solution was removed and formazan crystals were dissolved in DMSO. A microplate reader (Bio-RAD 680, USA) recorded the optical density in a spectrophotometer at a stimulus wavelength of 540 nm. DMSO was served as a blank. The same numbers of cells in contact with culture media were supposed as the control groups.

2.12 Cell Attachment and DAPI Staining

DAPI or 4′, 6-diamidino-2-phenylindole was used as nuclear stain. HFFF2 cells were seeded on the bandages (nanocomposite scaffolds with 0.5%, 1.5%, and 3.0% TiO_2 NPs), chitin and silk/fibroin as the control at a density of 10,000 cells and kept for 24 h of incubation. After

incubation, the cell seeded wells were washed with PBS and fixed with 4% paraformaldehyde for 20 min, permeabilised with 0.5% Triton X-100 (in PBS) for 15 min. The samples were washed with PBS and stained with 50 μL of DAPI and incubated in the dark for 5 min. The bandages were then washed with PBS and viewed under a fluorescent microscope (Olympus microscope Bh2-RFCA, Japan).

Statistical analysis

Statistical analysis was performed using SPSS v.16.0 software. Data were expressed as the mean ± significant if values obtained from the test were less than 0.05. (< 0.05) [43].

3. Results and discussion

3.1 FT-IR studies

Fig. 3A shows the FT-IR spectra of the prepared samples. Pure chitin showed characteristic peaks of -OH and amid I C=O stretching at 3436 and 1633 cm^{-1} respectively [14]. Pure silk fibroin showed the peaks at 1637 cm^{-1} (amid II), 1533 cm^{-1} (amid II) and 1264 cm^{-1} (amid III) which are characteristic of the silk I structural form (random coil and α-helix) [10]. FT-IR spectra of the chitin/silk fibroin showed the characteristic peaks of the pure materials [44, 45]. In FT-IR spectra of the nanocomposites containing different percentages of TiO_2, there was no significant difference with chitin/silk fibroin, whereas, the peak at 3420 cm^{-1} which is related to the stretching vibration of hydroxyl bond (-OH) are increased by enhancing amount of TiO_2 NPs concentration. It might be attributed to the presence of hydroxyl groups on the surface of NPs and by increasing TiO_2 content results to more adsorbed water with hydrophilic surface [46]. On

the hand, there are no differences between nanocomposite with various concentrations of TiO_2 NPs and it could be due to the low concentration of TiO_2 NPs.

3.2 XRD analysis

The XRD patterns of the prepared samples are presented in Fig. 3B. The XRD patterns of pure chitin and silk fibroin showed their characteristic peaks at 10 and 22.5° [20, 47]. The addition of chitin into silk fibroin did not change the position of the peaks of the related components, but the intensity of the peaks were decreased [11, 48]. It is reported that in the literature this is due to the penetration of silk fibroin first into the spaces between the chitin sheets, and then between the chitin chains [49]. This indicates mixing chitin and silk fibroin increased the crystalinty of the blend which could be attributed to the interactions available between chitin and silk fibroin [50]. Samples containing TiO_2 showed peaks around 20-25° and 29°. The addition of TiO_2 decreased the silk fibroin and chitin characteristic peaks intensity except 10° [51, 52].

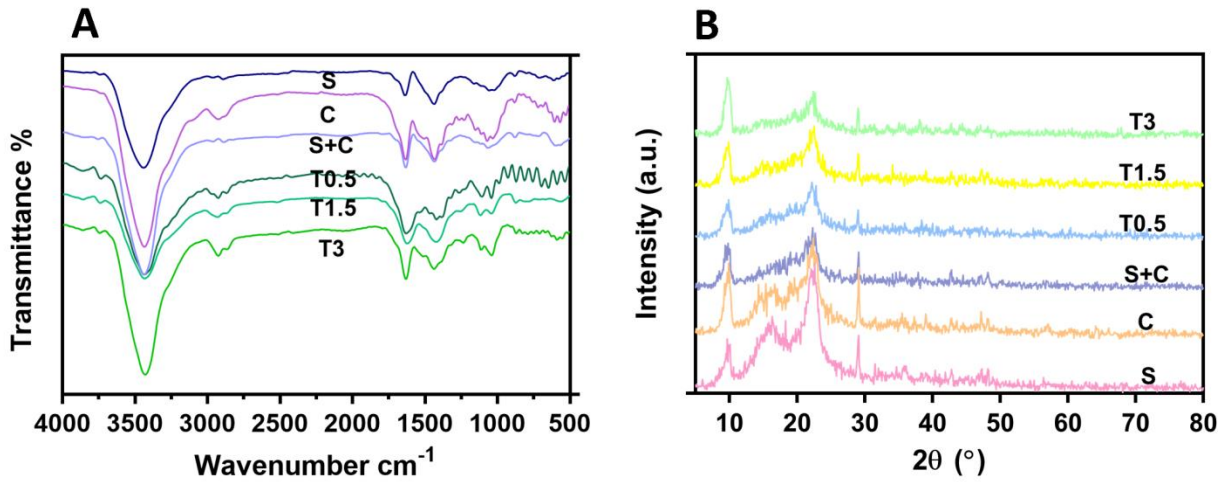

Fig.3 XRD paterns and FT-IR spectra of the pure silk fibroin (S), the pure chitin (C), the chitin/silk fibroin (S+C), the chitin/silk fibroin/TiO_2 (0.5 %) (T0.5), the chitin/silk fibroin/TiO_2 (1.5 %) (T1.5) and the chitin/silk fibroin/TiO_2 (3.0 %) (T3).

3.3 Scanning Electron Microscope (SEM) analysis

SEM images of the pure chitin and pure silk fibroin showed a layered morphology (Fig. 4a). As it can be seen the addition of TiO_2 NPs resulted in a homogenous 3D porous structure with rough pore wall suitable for cell penetration, growth and adhesion [53, 54]. Moreover, it can be seen increasing TiO_2 concentration resulted in a decrease in pore size. This could be attributed to the possible interactions between polymer matrix and TiO_2 NPs and exit of the water of the TiO_2 suspension used in the nanocomposite preparation process during the freeze-drying resulted in homogenous pores [54]. There was no sign of agglomeration of the NPs. Using the software "Image J", SEM micrographs was analyzed to study the pores of the samples (Fig. 4b). Four images with different magnification for each sample was analyzed with the software and the obtained data was statistically evaluated. Results are reported in table 1. Mean and maximum pore diameter were 100-150 μm and 150-250 μm respectively, which is suitable for wound dressing applications [13]. Moreover, it is reported pores smaller than 160 μm is ideal for dermal fibroblast growth [52, 54]. It can be seen increasing NPs content resulted in a decrease in pore diameter.

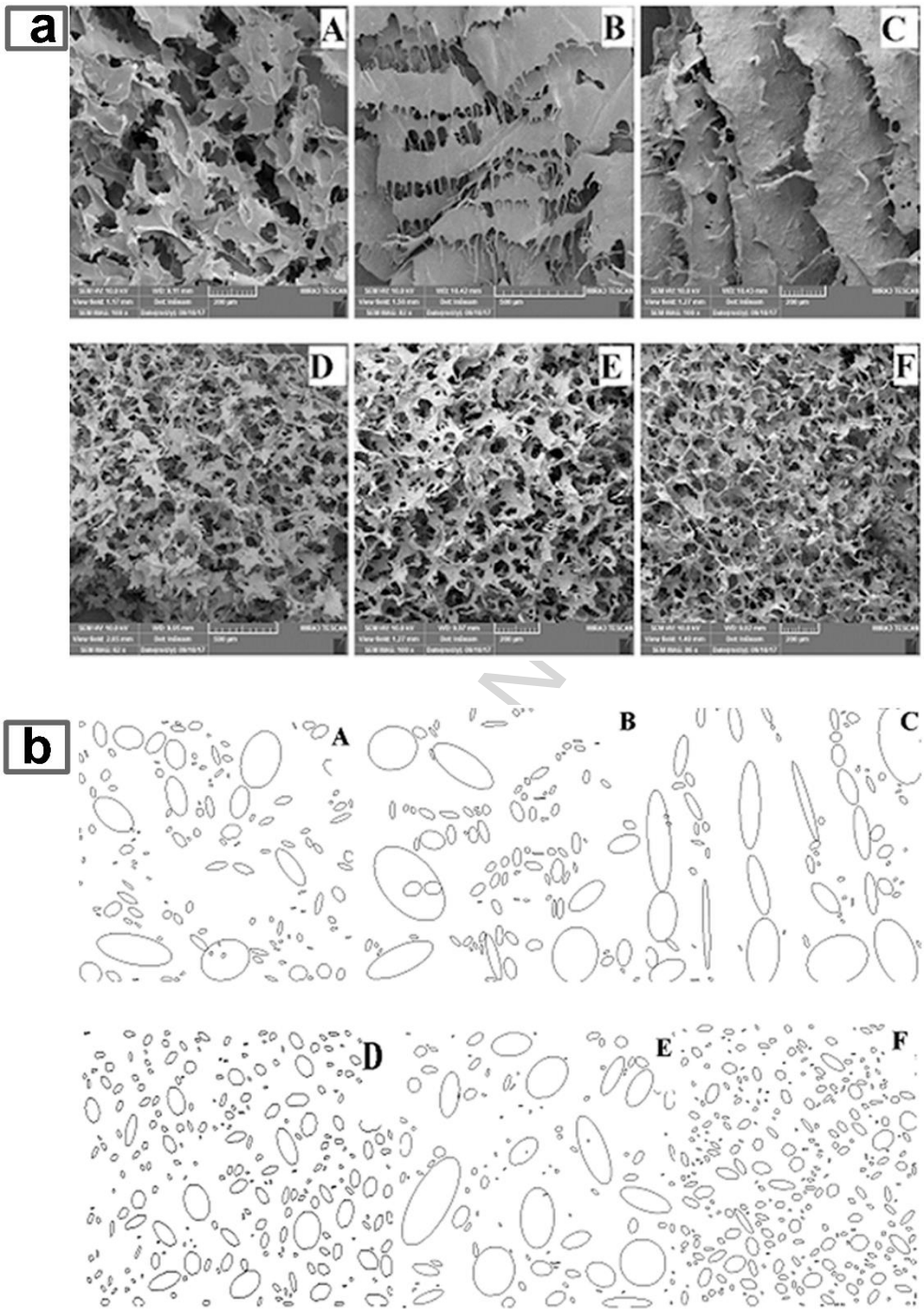

Fig. 4 **(a)** SEM images and of the pure chitin (A), pure silk fibroin (B), chitin/silk fibroin/TiO_2 (0.5 %) (C), chitin/silk fibroin/TiO_2 (1.5 %) (D) and chitin/silk fibroin/TiO_2 (3.0 %) (E). **(b)** Pore size of the prepared nanocomposites determined using SEM images and "Image J" software.

Table 1. Porosity, density, and average pores diameter.

Comp	Average of Feret's diameter (µm)	Average of Maximum Feret's Diameter (µm)	porosity (%)	Density (mg/ml)
C *	166.44	337.42	96.38554	1673.378
S	176.53	414.75	96.97987	1717.031
S+C *	218.94	473.85	97.03116	1859.632
T 0.5	148.32	255.32	94.99136	2801.089
T 1.5	113.51	247.25	94.07008	3118.561
T 3.0	113.04	168.42	93.92477	3720.083

*** Layer**

3.4 Porosity and density

Porosity is one of the most important key factors determining the cell growth [54]. The porosity and the density of the samples are summarized in table 1. All of the samples showed porosity above 90 %, which is suitable for cell growth, cell immigration and cell attachment. Moreover, the porous structure of the samples is necessary for wound exudates secretion and delivery of the oxygen and nutrients [55]. Nonetheless, high porosity leads to low mechanical properties [56]. This problem could be controlled by freeze-drying process parameters like temperature and rate of cooling, which control ice crystal growth [39]. It can be seen the addition of TiO_2 NPs decreased the porosity and increase of the TiO_2 percent decreased the porosity of the sample.

3.5 *In-vitro* swelling and degradation studies

The swelling degree of the prepared nanocomposite dressings is presented in Fig. 5A. Silk fibroin completely dissolved in PBS. All the other samples showed a swelling degree above 93%. Moreover, samples were saturated during the first 24 h and increase of the immersion time after 24 h had not salient effect on swelling. The high swelling degree of the prepared dressings

is necessary for wound dressing and highly helpful in absorbing wound exudates and preventing wound infections, which could accelerate wound healing [14, 47]. As it can be seen, increase of the TiO_2 NPs slightly decreased the swelling. This is related to the available interactions between TiO_2 and chitin/silk fibroin [57].

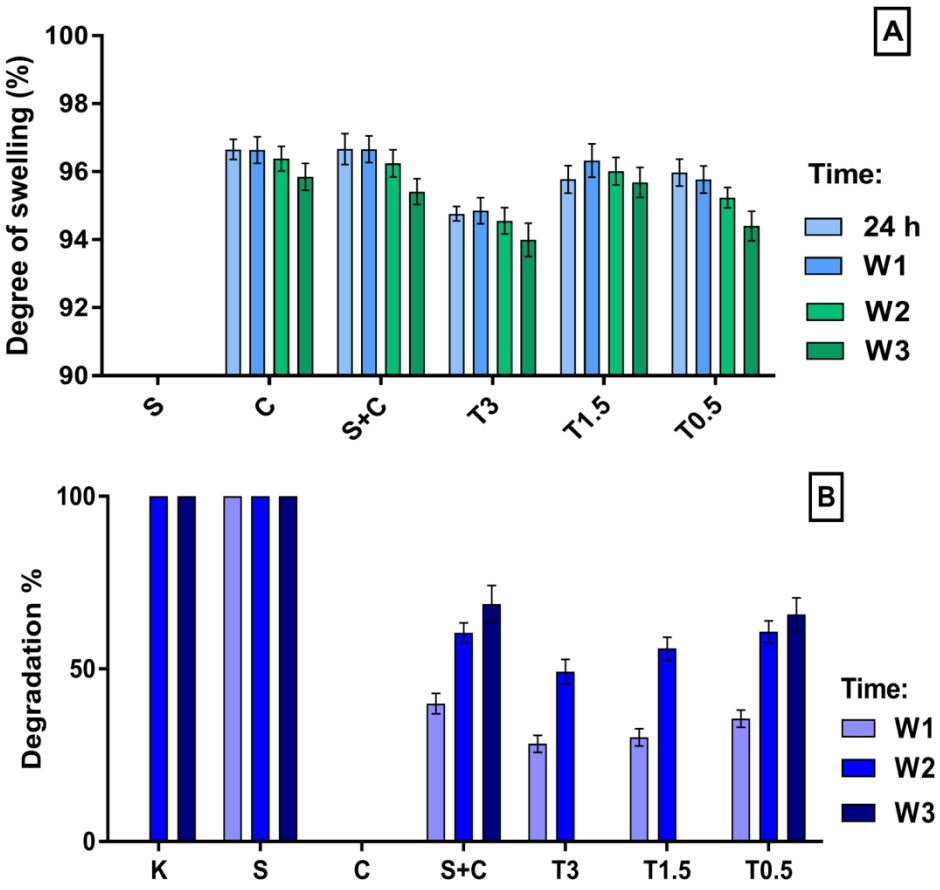

Fig. 5. Degree of swelling (A), and degradation (B) of prepared dressings after 24 h, one, two, and three weeks.

An ideal wound dressing should have biodegrading rate proportional to tissue healing rate [58]. It is reported that lysozyme degradation products of chitin are nontoxic glucosamine and N-acetyl glucosamine and could accelerate healing through direction keratinocyte to the wound area [55]. Biodegradation products of silk fibroin are amino acids like glycine and alanine, which

have significant impact on angiogenesis [55]. *In-vitro* biodegradation results (Fig. 5B) showed degradation of the prepared dressings could be controlled by adjusting of the components' percentage. Silk fibroin dissolved at the first moments. Unexpectedly, pure chitin had high durability and did not show any weight loss during 21 days. The control calcium alginate dressing did not show noticeable weight loss within the first week but then it was completely dissolved during the next weeks. Chitin/silk fibroin/ TiO_2 nanocomposite showed an appropriate biodegradation rate. Within firs the week nanocomposite degradation was between 30-40% and during second and third week degradation reached at 50-60% and 60-70% respectively. Within the first and the second weeks, increasing TiO_2 content decreased biodegradation of the sample. As it can be seen, on the last week sample containing 0.5 % TiO_2 showed 67 % degradation, but dressings with higher amount of TiO_2 were dissolved completely. This showed TiO_2 concentrations higher than 0.5 % weakens interactions available between polymer chains.

3.6 Mechanical properties

Fig. 6 displays results of the mechanical properties. SF is a fibrous protein with high tensile strength and flexibility. CS is a crystalline polysaccharide, with structure similar to glycosaminoglycans. It can be seen both elongation at break and tensile strength of chitin/silk fibroin composite was improved in comparison to pure components. This is could be related to the possible H-bonding between available amid groups in chitin and silk fibroin [12]. Chitin is a good additive to improve silk fibroin mechanical properties. Chitin fills unoccupied areas available in amorphous silk fibroin increasing its crystallinity [50, 59]. Most of the available studies indicated that addition of proteins (silk fibroin) into polysaccharides (chitin) increases the flexibility of the resulted composite which is due to the participation of hydrophilic groups. As it can be seen, low concentration of TiO_2 NPs did not change mechanical properties. Increase of

the TiO_2 concentration dramatically deteriorated tensile strength and elongation at break. This is related to damage of microscopic structure of the sponges due to the formation of TiO_2 agglomerations [45]. Moreover, it could be related to the extra water used for NPs suspension creation which was weekend strength of the dressings.

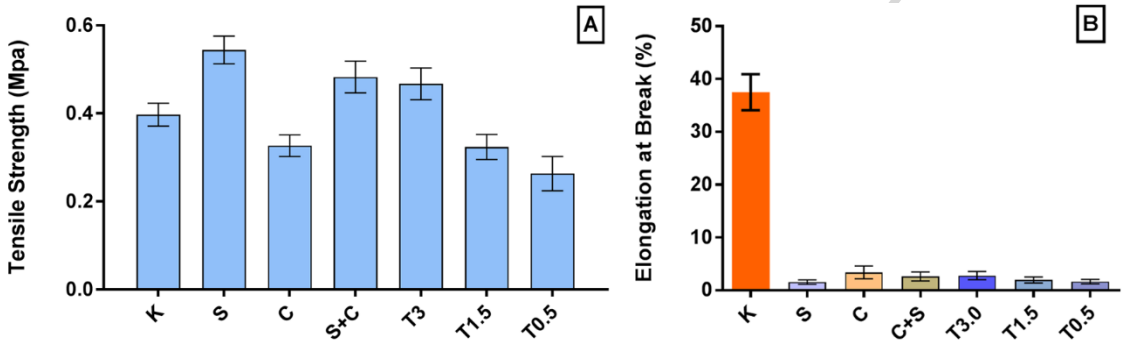

Fig. 6 Tensile strength (A) and elongation at break (B) of the prepared dressings.

3.7 Blood clotting analysis

The results of the blood clotting study are represented in Fig. 7. Chitin and silk fibroin showed much higher blood clotting ability compared to control Kaltostat and pure blood. This is related to the cationic nature of the used polymers and negatively charged blood cells [60, 61]. The addition of chitin to the silk fibroin was improved blood clotting ability compared to the pure polymers, positive and negative controls. TiO_2 NPs did not have a significant impact on the blood clotting ability and merely increased optical density.

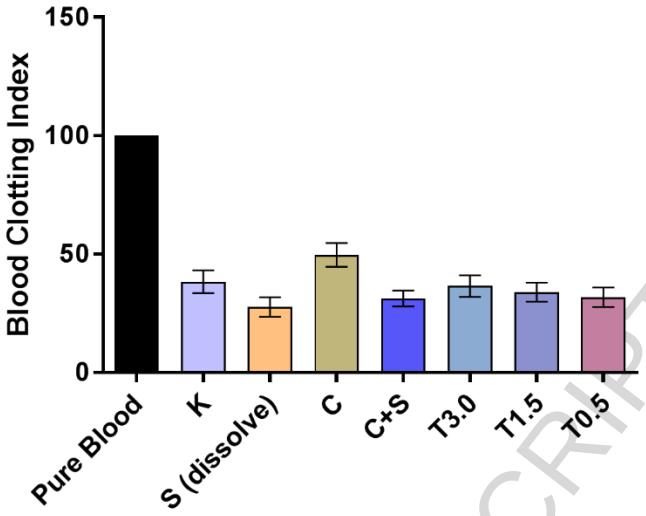

Fig. 7 Blood clotting studies of the prepared dressings.

3.8 *In-vitro* antibacterial and antifungal activities evaluation

Fig. 8 represents the antibacterial and antifungal activities of the dressings determined using the disk diffusion method. As reported on previously published papers, pure chitin, pure silk fibroin and chitin/silk fibroin composite without TiO_2 NPs did not show any inhibition zone [62]. TiO_2 containing dressings showed salient antibacterial and antifungal activities against all strains. The interactions available between TiO_2 and polymer matrix is of physical type resulting in controlled release of TiO_2 NPs [63]. Moreover, high swelling properties of the dressing could help the release of the TiO_2 NPs and hence had an effective role in the observed antibacterial and antifungal activities [64]. Due to electrostatic interactions, TiO_2 NPs stick to the bacterial cell wall resulting in a morphological change and cell wall material transfer disturbance and finally cell death [65]. Viewed inhibition zone of plates containing *C. albicans* was the biggest and *S. aureus* was the smallest. This can be attributed to the presence of a thick layer of peptido glycans

in the cell wall of gram positive strains which prohibit TiO_2 NPs penetration [3]. It is viewed increase of TiO_2 concentration did not change the zone of inhibition.

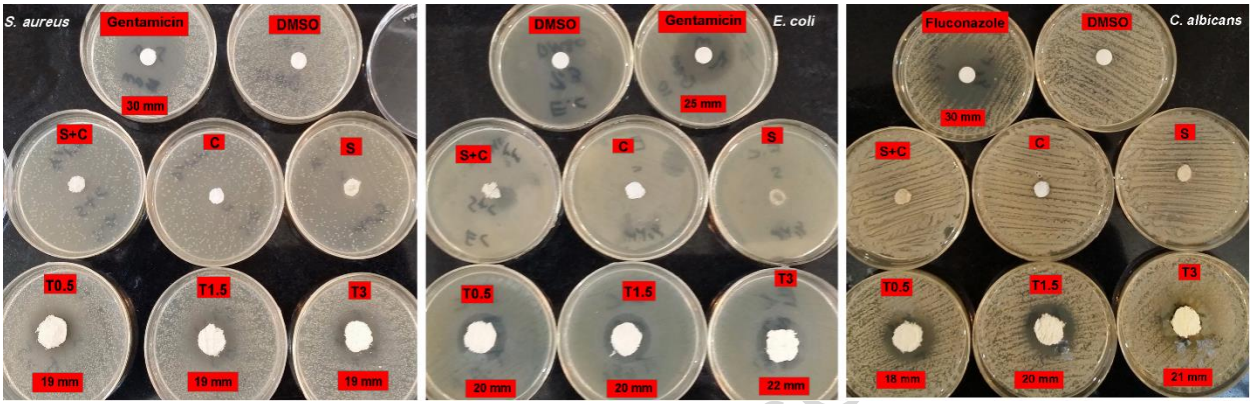

Fig. 8 Photographs of the inhibition zone of the prepared nanocomposite dressing against *C. albicans*, *E. coli*, and *S. aureus* using disk diffusion method.

Colony count method (Fig. 9) was used to more accurately study the antibacterial and antifungal properties of the prepared dressing, especially in 3D mode [66]. Results were consistent with the disk diffusion. As it can be seen, chitin/silk fibroin had the greatest antibacterial and antifungal activities compared to pure chitin and pure silk fibroin. In dressing with the highest percentage of TiO_2, the number of colonies was reduced about 5 fold compared to control sample without TiO_2.

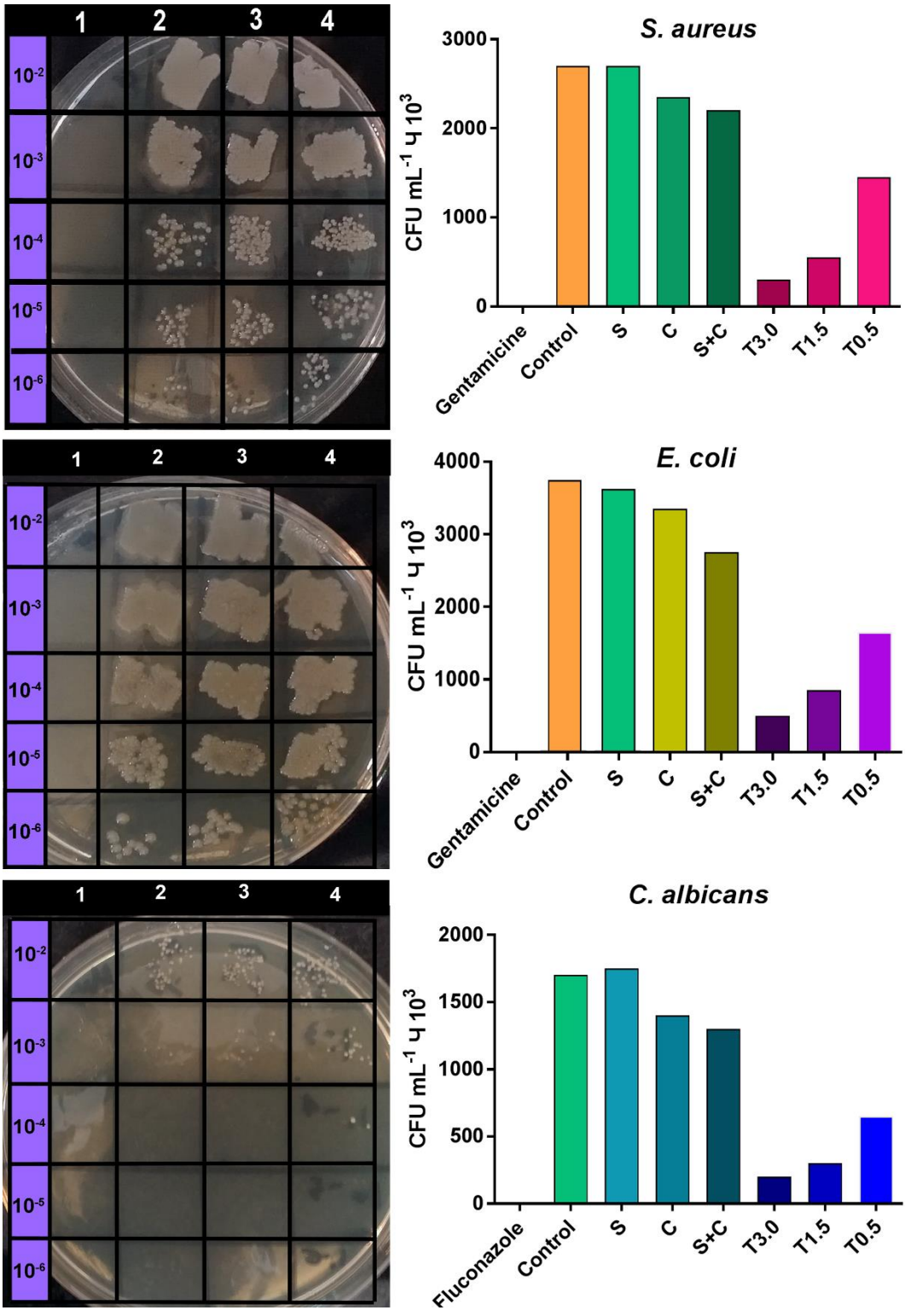

Fig. 9 Colony count evaluation of Gentamicin as a positive control (column 1), nanocomposites with 0.5% TiO_2 (column 2), 1.5% TiO_2 (column 3), and 3.0% TiO_2 (column 4) against *C. albicans*, *E. coli*, and *S. aureus*

3.9 Cell viability evaluation

Due to the prepared nanocomposites were designed to use for wound dressing applications, the normal human dermal fibroblast (HFFF2) cells were chosen for biological applications. The cell viability and proliferation as a function of time on a scaffold are indicative of the cellular compatibility and appropriateness for tissue engineering applications are reported for their good biocompatibility [60]. Cell viability results (Fig. 10A) revealed that both silk fibroin and chitin had viability of below 25% for 24 and 48 h incubation. In nanocomposite scaffolds containing TiO_2 NPs with increasing the TiO_2 NPs content from 0.5 to 1.5 and 3.0% the viability of HFFF2 was decreased with time dependent manner. Nanocomposite scaffolds with 3.0% TiO_2 NPs had the lowest cell viability, which indicating the cytotoxicity of TiO_2 NPs at higher concentrations. This result suggests the suitability of this bandage containing 0.5 to 1.5 TiO_2 NPs for tissue engineering applications and non-cytotoxic nature of the blends.

3.10 Cell attachment study by DAPI staining

DAPI staining of the HFFF2 cells attached on the bandages was confirmed by the cyto-compatible nature of the bandages (Fig. 10C). By investigating the DAPI staining analysis images, we found that the nanocomposite bandages with lower TiO_2 concentration has higher number of cell attachments. By more evaluation, it was seen that the nanocomposites containing 3.0 wt% TiO_2 has low cell growth. The cytotoxicity could be either due to endocytosis of TiO_2 or cellular membrane damage by the interaction with TiO_2. It also attributed the toxic effect of TiO_2

at higher concentration. However, lower doses of TiO_2 NPs (0.5 and 1.5%) have positive effects on cell attachment and proliferation.

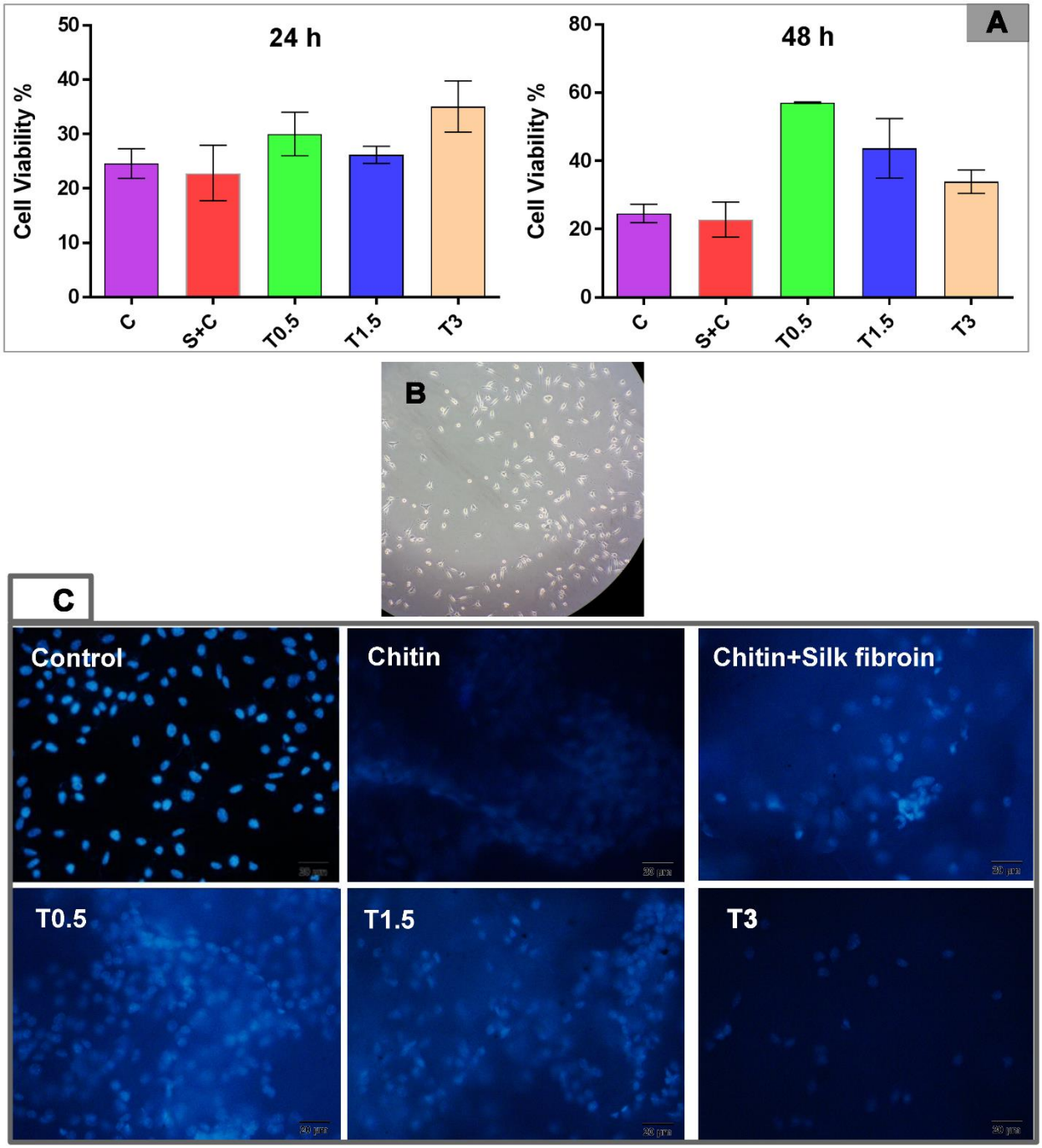

Fig. 10 (A) Proliferation and cell viability of HFFF2 cell cultured on chitin, silk fibroin/chitin, and scaffolds with different TiO_2 NPs contents after 24 and 48 h. (B) Microscopic photograph of

the HFFF2 cells. (C) DAPI staining of the HFFF2 cells attached on the chitin, silk fibroin/chitin, and nanocomposite scaffolds with 0.5%, 1.5%, and 3.0% TiO_2 NPs. The cells with no treatment used as a control.

4. Conclusion

A novel silk fibroin/chitin/TiO_2 NPs scaffolds were prepared using freeze-drying method. The prepared nanocomposites were characterized by SEM, FTIR and XRD analysis. It was proven due to possible inter-chain interactions, the addition of chitin to silk fibroin greatly improved silk fibroin biodegradation. The addition of TiO_2 NPs even at low percentage (0.5 %) showed good antibacterial and antifungal activities. The cytotoxicity assay and cell attachment by MTT assay and DAPI staining evaluation of scaffolds on HFFF2 cells were performed. Good biocompatibility, biodegradability, blood clotting capability, and water-uptake ability results have shown that the prepared scaffold has a good potential for wound dressing applications.

Acknowledgment

We thank Drug Applied Research Center (DARC) of Tabriz University of Medical Sciences. All experiments were done in Microbiology laboratory of DARC and financially supported by DARC.

References

[1] D. Liang, Z. Lu, H. Yang, J. Gao, R. Chen, Novel asymmetric wettable AgNPs/chitosan wound dressing: in vitro and in vivo evaluation, ACS applied materials & interfaces 8(6) (2016) 3958-3968.
[2] A.A. Chaudhari, K. Vig, D.R. Baganizi, R. Sahu, S. Dixit, V. Dennis, S.R. Singh, S.R. Pillai, Future Prospects for Scaffolding Methods and Biomaterials in Skin Tissue Engineering: A Review, International Journal of Molecular Sciences 17(12) (2016).
[3] P.T. Kumar, V.K. Lakshmanan, T.V. Anilkumar, C. Ramya, P. Reshmi, A.G. Unnikrishnan, S.V. Nair, R. Jayakumar, Flexible and microporous chitosan hydrogel/nano ZnO composite bandages for wound dressing: in vitro and in vivo evaluation, ACS Appl Mater Interfaces 4(5) (2012) 2618-29.
[4] Z. Lu, J. Gao, Q. He, J. Wu, D. Liang, H. Yang, R. Chen, Enhanced antibacterial and wound healing activities of microporous chitosan-Ag/ZnO composite dressing, Carbohydrate polymers 156 (2017) 460-469.
[5] F. Wahid, J.-J. Yin, D.-D. Xue, H. Xue, Y.-S. Lu, C. Zhong, L.-Q. Chu, Synthesis and characterization of antibacterial carboxymethyl Chitosan/ZnO nanocomposite hydrogels, International Journal of Biological Macromolecules 88 (2016) 273-279.
[6] M.G. Mehrabani, R. Karimian, B. Mehramouz, M. Rahimi, H.S. Kafil, Preparation of biocompatible and biodegradable silk fibroin/chitin/silver nanoparticles 3D scaffolds as a bandage for antimicrobial wound dressing, International journal of biological macromolecules 114 (2018) 961-971.
[7] J.-P. Chen, Y. Chiang, Bioactive electrospun silver nanoparticles-containing polyurethane nanofibers as wound dressings, Journal of nanoscience and nanotechnology 10(11) (2010) 7560-7564.
[8] H.R. Ashjari, M.S.S. Dorraji, V. Fakhrzadeh, H. Eslami, M.H. Rasoulifard, M. Rastgouy-Houjaghan, P. Gholizadeh, H.S. Kafil, Starch-based polyurethane/CuO nanocomposite foam: Antibacterial effects for infection control, Int J Biol Macromol 21(17) (2018) 34569-5.
[9] S. Kumbar, C. Laurencin, M. Deng, Natural and synthetic biomedical polymers, Newnes2014.
[10] M. Azadi, A. Teimouri, G. Mehranzadeh, Preparation, characterization and biocompatible properties of β-chitin/silk fibroin/nanohydroxyapatite composite scaffolds prepared using a freeze-drying method, RSC Advances 6(9) (2016) 7048-7060.
[11] H.O. Barud, H.d.S. Barud, M. Cavicchioli, T.S. do Amaral, O.B. de Oliveira Junior, D.M. Santos, A.L.d.O.A. Petersen, F. Celes, V.M. Borges, C.I. de Oliveira, Preparation and characterization of a bacterial cellulose/silk fibroin sponge scaffold for tissue regeneration, Carbohydrate polymers 128 (2015) 41-51.
[12] J. Jin, P. Hassanzadeh, G. Perotto, W. Sun, M.A. Brenckle, D. Kaplan, F.G. Omenetto, M. Rolandi, A Biomimetic Composite from Solution Self-Assembly of Chitin Nanofibers in a Silk Fibroin Matrix, Advanced Materials 25(32) (2013) 4482-4487.
[13] Z. Karahaliloglu, E. Kilicay, E.B. Denkbas, Antibacterial chitosan/silk sericin 3D porous scaffolds as a wound dressing material, Artificial cells, nanomedicine, and biotechnology 45(6) (2017) 1172-1185.
[14] S. Li, L. Li, C. Guo, H. Qin, X. Yu, A promising wound dressing material with excellent cytocompatibility and proangiogenesis action for wound healing: Strontium loaded Silk

fibroin/Sodium alginate (SF/SA) blend films, International journal of biological macromolecules 104 (2017) 969-978.
[15] D.M. Phillips, L.F. Drummy, D.G. Conrady, D.M. Fox, R.R. Naik, M.O. Stone, P.C. Trulove, H.C. De Long, R.A. Mantz, Dissolution and regeneration of Bombyx mori silk fibroin using ionic liquids, Journal of the American Chemical Society 126(44) (2004) 14350-14351.
[16] E. Sashina, A. Bochek, N. Novoselov, D. Kirichenko, Structure and solubility of natural silk fibroin, Russian Journal of Applied Chemistry 79(6) (2006) 869-876.
[17] R. Jayakumar, V.D. Rani, K. Shalumon, P.S. Kumar, S. Nair, T. Furuike, H. Tamura, Bioactive and osteoblast cell attachment studies of novel α-and β-chitin membranes for tissue-engineering applications, International journal of biological macromolecules 45(3) (2009) 260-264.
[18] R. Tajiri, A. Mihata, K. Yamamoto, J.-i. Kadokawa, Facile preparation of chitin gels with calcium bromide dihydrate/methanol media and their efficient conversion into porous chitins, RSC Advances 4(11) (2014) 5542-5546.
[19] Y. Maeda, R. Jayakumar, H. Nagahama, T. Furuike, H. Tamura, Synthesis, characterization and bioactivity studies of novel β-chitin scaffolds for tissue-engineering applications, International journal of biological macromolecules 42(5) (2008) 463-467.
[20] H. Tamura, H. Nagahama, S. Tokura, Preparation of chitin hydrogel under mild conditions, Cellulose 13(4) (2006) 357-364.
[21] R. Jayakumar, M. Prabaharan, S. Nair, H. Tamura, Novel chitin and chitosan nanofibers in biomedical applications, Biotechnology advances 28(1) (2010) 142-150.
[22] R. Jayakumar, M. Prabaharan, P.S. Kumar, S. Nair, H. Tamura, Biomaterials based on chitin and chitosan in wound dressing applications, Biotechnology advances 29(3) (2011) 322-337.
[23] K. Azuma, R. Izumi, T. Osaki, S. Ifuku, M. Morimoto, H. Saimoto, S. Minami, Y. Okamoto, Chitin, chitosan, and its derivatives for wound healing: old and new materials, Journal of functional biomaterials 6(1) (2015) 104-142.
[24] V. Patrulea, V. Ostafe, G. Borchard, O. Jordan, Chitosan as a starting material for wound healing applications, European Journal of Pharmaceutics and Biopharmaceutics 97 (2015) 417-426.
[25] A.L. Harkins, S. Duri, L.C. Kloth, C.D. Tran, Chitosan–cellulose composite for wound dressing material. Part 2. Antimicrobial activity, blood absorption ability, and biocompatibility, Journal of Biomedical Materials Research Part B: Applied Biomaterials 102(6) (2014) 1199-1206.
[26] W.M. Kirsch, S. Hudson, Chitosan-based hemostatic textile, Google Patents, 2016.
[27] S.-H. Chang, H.-T.V. Lin, G.-J. Wu, G.J. Tsai, pH Effects on solubility, zeta potential, and correlation between antibacterial activity and molecular weight of chitosan, Carbohydrate polymers 134 (2015) 74-81.
[28] F.B. zeynabad, R. Salehi, E. Alizadeh, H.S. Kafil, A. Hassanzadeh, M. Mahkam, pH-Controlled multiple-drug delivery by a novel antibacterial nanocomposite for combination therapy, RSC advances 5(128) (2015) 105678-105691.
[29] R.R. Mohamed, M.W. Sabaa, Synthesis and characterization of antimicrobial crosslinked carboxymethyl chitosan nanoparticles loaded with silver, International Journal of Biological Macromolecules 69 (2014) 95-99.

[30] P. Petkova, A. Francesko, M.M. Fernandes, E. Mendoza, I. Perelshtein, A. Gedanken, T. Tzanov, Sonochemical coating of textiles with hybrid ZnO/chitosan antimicrobial nanoparticles, ACS applied materials & interfaces 6(2) (2014) 1164-1172.
[31] S. Kumar-Krishnan, E. Prokhorov, M. Hernández-Iturriaga, J.D. Mota-Morales, M. Vázquez-Lepe, Y. Kovalenko, I.C. Sanchez, G. Luna-Bárcenas, Chitosan/silver nanocomposites: Synergistic antibacterial action of silver nanoparticles and silver ions, European Polymer Journal 67 (2015) 242-251.
[32] R.E. Morsi, A.M. Alsabagh, S.A. Nasr, M.M. Zaki, Multifunctional nanocomposites of chitosan, silver nanoparticles, copper nanoparticles and carbon nanotubes for water treatment: Antimicrobial characteristics, International journal of biological macromolecules 97 (2017) 264-269.
[33] S. Ferraris, S. Spriano, Antibacterial titanium surfaces for medical implants, Materials Science and Engineering: C 61 (2016) 965-978.
[34] M.E. El-Naggar, T.I. Shaheen, S. Zaghloul, M.H. El-Rafie, A. Hebeish, Antibacterial activities and UV protection of the in situ synthesized titanium oxide nanoparticles on cotton fabrics, Industrial & Engineering Chemistry Research 55(10) (2016) 2661-2668.
[35] Y. Haldorai, J.J. Shim, Novel chitosan-TiO2 nanohybrid: Preparation, characterization, antibacterial, and photocatalytic properties, Polymer Composites 35(2) (2014) 327-333.
[36] N. Johari, H.M. Hosseini, A. Samadikuchaksaraei, Optimized composition of nanocomposite scaffolds formed from silk fibroin and nano-TiO 2 for bone tissue engineering, Materials Science and Engineering: C 79 (2017) 783-792.
[37] B. Li, Y. Zhang, Y. Yang, W. Qiu, X. Wang, B. Liu, Y. Wang, G. Sun, Synthesis, characterization, and antibacterial activity of chitosan/TiO2 nanocomposite against Xanthomonas oryzae pv. oryzae, Carbohydrate Polymers 152 (2016) 825-831.
[38] J.-H. Kim, F.A. Sheikh, H.W. Ju, H.J. Park, B.M. Moon, O.J. Lee, C.H. Park, 3D silk fibroin scaffold incorporating titanium dioxide (TiO2) nanoparticle (NPs) for tissue engineering, International Journal of Biological Macromolecules 68 (2014) 158-168.
[39] R. Nazarov, H.-J. Jin, D.L. Kaplan, Porous 3-D scaffolds from regenerated silk fibroin, Biomacromolecules 5(3) (2004) 718-726.
[40] H.S. Kafil, A.M. Mobarez, Spread of Enterococcal Surface Protein in Antibiotic Resistant Entero-coccus faecium and Enterococcus faecalis isolates from Urinary Tract Infections, Open Microbiol J 9 (2015) 14-7.
[41] M. Aghazadeh, A. Zahedi Bialvaei, F. Kabiri, N. Saliani, M. Yousefi, H. Eslami, H. Samadi Kafil, Survey of the Antibiofilm and Antimicrobial Effects of Zingiber officinale (in Vitro Study), Jundishapur J Microbiol 9(2) (2016).
[42] E. Zakerzadeh, E. Alizadeh, H. Samadi Kafil, A. Mohammad Hassanzadeh, R. Salehi, M. Mahkam, Novel antibacterial polymeric nanocomposite for smart co-delivery of anticancer drugs, Artif Cells Nanomed Biotechnol 45(8) (2017) 1509-1520.
[43] M. Asgharzadeh, K. Shahbabian, H.S. Kafil, A. Rafi, Use of DNA Fingerprinting in Identifying the Source Case of Tuberculosis in East Azarbaijan Province of Iran, J. Med. Sci 7(3) (2007) 418-421.
[44] R. Jayakumar, R. Ramachandran, V. Divyarani, K. Chennazhi, H. Tamura, S. Nair, Fabrication of chitin–chitosan/nano TiO 2-composite scaffolds for tissue engineering applications, International journal of biological macromolecules 48(2) (2011) 336-344.

[45] Q. He, Y. Zhang, X. Cai, S. Wang, Fabrication of gelatin–TiO 2 nanocomposite film and its structural, antibacterial and physical properties, International journal of biological macromolecules 84 (2016) 153-160.
[46] V. Bolis, C. Busco, M. Ciarletta, C. Distasi, J. Erriquez, I. Fenoglio, S. Livraghi, S. Morel, Hydrophilic/hydrophobic features of TiO2 nanoparticles as a function of crystal phase, surface area and coating, in relation to their potential toxicity in peripheral nervous system, Journal of colloid and interface science 369(1) (2012) 28-39.
[47] G. Li, W. Li, H. Deng, Y. Du, Structure and properties of chitin/alginate blend membranes from NaOH/urea aqueous solution, International journal of biological macromolecules 51(5) (2012) 1121-1126.
[48] B.J. Allardyce, R. Rajkhowa, R.J. Dilley, S.L. Redmond, M.D. Atlas, X. Wang, Glycerol-plasticised silk membranes made using formic acid are ductile, transparent and degradation-resistant, Materials Science and Engineering: C 80 (2017) 165-173.
[49] G. Falini, S. Weiner, L. Addadi, Chitin-silk fibroin interactions: relevance to calcium carbonate formation in invertebrates, Calcified tissue international 72(5) (2003) 548-554.
[50] F.I. Khan, S. Rahman, A. Queen, S. Ahamad, S. Ali, J. Kim, M.I. Hassan, Implications of molecular diversity of chitin and its derivatives, Applied microbiology and biotechnology 101(9) (2017) 3513-3536.
[51] S.S. Behera, U. Das, A. Kumar, A. Bissoyi, A.K. Singh, Chitosan/TiO 2 composite membrane improves proliferation and survival of L929 fibroblast cells: Application in wound dressing and skin regeneration, International Journal of Biological Macromolecules 98 (2017) 329-340.
[52] N. Johari, H.R.M. Hosseini, A. Samadikuchaksaraei, Novel fluoridated silk fibroin/TiO2 nanocomposite scaffolds for bone tissue engineering, Materials Science and Engineering: C 82 (2018) 265-276.
[53] A. Teimouri, M. Azadi, β-Chitin/gelatin/nanohydroxyapatite composite scaffold prepared through freeze-drying method for tissue engineering applications, Polymer Bulletin 73(12) (2016) 3513-3529.
[54] A. Teimouri, M. Azadi, Z. Shams Ghahfarokhi, R. Razavizadeh, Preparation and characterization of novel β-chitin/nanodiopside/nanohydroxyapatite composite scaffolds for tissue engineering applications, Journal of Biomaterials Science, Polymer Edition 28(1) (2017) 1-14.
[55] P. Kumar, V.-K. Lakshmanan, R. Biswas, S.V. Nair, R. Jayakumar, Synthesis and biological evaluation of chitin hydrogel/nano ZnO composite bandage as antibacterial wound dressing, Journal of biomedical nanotechnology 8(6) (2012) 891-900.
[56] B. Zdravkov, J. Čermák, M. Šefara, J. Janků, Pore classification in the characterization of porous materials: A perspective, Open Chemistry 5(2) (2007) 385-395.
[57] R. Jayakumar, R. Ramachandran, P.S. Kumar, V. Divyarani, S. Srinivasan, K. Chennazhi, H. Tamura, S. Nair, Fabrication of chitin–chitosan/nano ZrO 2 composite scaffolds for tissue engineering applications, International journal of biological macromolecules 49(3) (2011) 274-280.
[58] S. Srinivasan, P. Kumar, S.V. Nair, S.V. Nair, K. Chennazhi, R. Jayakumar, Antibacterial and bioactive α-and β-chitin hydrogel/nanobioactive glass ceramic/nano silver composite scaffolds for periodontal regeneration, Journal of biomedical nanotechnology 9(11) (2013) 1803-1816.

[59] K.G. Lee, H. Kweon, J.H. Yeo, S.O. Woo, J.H. Lee, Y. Hwan Park, Structural and physical properties of silk fibroin/alginate blend sponges, Journal of applied polymer science 93(5) (2004) 2174-2179.
[60] K. Madhumathi, P.S. Kumar, S. Abhilash, V. Sreeja, H. Tamura, K. Manzoor, S. Nair, R. Jayakumar, Development of novel chitin/nanosilver composite scaffolds for wound dressing applications, Journal of Materials Science: Materials in Medicine 21(2) (2010) 807-813.
[61] R.A. Muzzarelli, Chitins and chitosans as immunoadjuvants and non-allergenic drug carriers, Marine drugs 8(2) (2010) 292-312.
[62] C.M. Srivastava, R. Purwar, A. Gupta, D. Sharma, Dextrose modified flexible tasar and muga fibroin films for wound healing applications, Materials Science and Engineering: C 75 (2017) 104-114.
[63] P.S. Kumar, S. Abhilash, K. Manzoor, S. Nair, H. Tamura, R. Jayakumar, Preparation and characterization of novel β-chitin/nanosilver composite scaffolds for wound dressing applications, Carbohydrate Polymers 80(3) (2010) 761-767.
[64] K. Karthikeyan, S. Sekar, M.P. Devi, S. Inbasekaran, C. Lakshminarasaiah, T. Sastry, Fabrication of novel biofibers by coating silk fibroin with chitosan impregnated with silver nanoparticles, Journal of Materials Science: Materials in Medicine 22(12) (2011) 2721-2726.
[65] P. Uttayarat, S. Jetawattana, P. Suwanmala, J. Eamsiri, T. Tangthong, S. Pongpat, Antimicrobial electrospun silk fibroin mats with silver nanoparticles for wound dressing application, Fibers and Polymers 13(8) (2012) 999-1006.
[66] X. Zhang, G. Xiao, Y. Wang, Y. Zhao, H. Su, T. Tan, Preparation of chitosan-TiO 2 composite film with efficient antimicrobial activities under visible light for food packaging applications, Carbohydrate Polymers 169 (2017) 101-107.

Graphical abstract